Available online at www.sciencedirect.com
SCIENCE DIRECT®
Biochemical and Biophysical Research Communications 328 (2005) 306–311
BBRC
www.elsevier.com/locate/ybbrc

Odd-skipped related 2 splicing variants show opposite transcriptional activity

Shinji Kawai*, Takahiro Kato, Hiroaki Inaba, Nobuo Okahashi, Atsuo Amano

Department of Oral Frontier Biology, Osaka University Graduate School of Dentistry, 1-8 Yamadaoka, Suita-Osaka 565-0871, Japan

Received 14 December 2004
Available online 7 January 2005

Abstract

Odd-skipped related 2 (Osr2) is expressed in the domain of epithelial–mesenchymal interactions during tooth and kidney development. In this study, we report that alternative splicing of exon 4 resulted in two transcripts, Osr2A and Osr2B. These variants utilized a different splice acceptor, and Osr2B exhibited a frameshift followed by an early stop codon. Osr2A mRNA produced a protein that was 36 amino acids longer than Osr2B at the C-terminus and had five zinc-finger domains, whereas Osr2B had three zinc-finger motives. The 2 Osr2 variants were found in kidney, skeletal muscle, and testis, and Osr2B was predominantly transcribed in each. Flag-tagged variants showed the same localization in cell nuclei, however, Gal4 fusion proteins showed opposite transcriptional activities. Further, Flag-tagged variants also showed opposite transcriptional activities, though they were in contrast to the findings for the Gal4-fused variants. Our results indicate that Osr2 bifurcates its function by alternative splicing.

Keywords: Odd-skipped related 2; Gene structure; Alternative splicing; Gene expression

The *Odd-skipped* gene was first identified as a part of *Drosophila* pair-rule transcription factors and shown to contain DNA-binding C2H2 type zinc-fingers in the C-terminal half of the molecule. Besides *Odd-skipped*, three genes in *Drosophila*, *brother of Odd with entrails limited* (*bowl*), *sister of Odd and bowl* (*sob*), and *drumstick* (*drm*), exhibit a homology in the zinc-finger domain of Odd-skipped, whereas no significant homology is displayed outside of this domain [1]. *Drosophila Odd-skipped* is primarily expressed in stripes that spread in even-numbered segments, and then later in narrow stripes in the center of both even- and odd-numbered segments [2,3]. Mutations in *Odd-skipped* cause pattern defects in the anterior regions of odd-numbered segments and partial substitution by mirror-image duplications in adjacent regions [4]. These defects are explained by changes in the expression levels of other segmentation genes, such as *fushi tarazu* (*ftz*), *engrailed* (*en*), and *wingless* (*wg*), by the *Odd-skipped* gene [5,6]. Thereafter, *Odd-skipped* genes were found in *Caenorhabditis elegans*, *Saccharomyces cerevisiae*, and *Xenopus laevis* [7–9].

Two mammalian homologs, *Osr1* and *Osr2*, from both mice and humans have been cloned [10–12]. Mammalian *Osr2* is expressed at sites of epithelial–mesenchymal interactions during limb, tooth, and kidney development, while mouse *Osr2* is observed in the mesonephric vesicles at E9.25. Further, *Osr2* is detected in the rostrolateral mandibular mesenchyme immediately neighboring the maxillary processes on E10.0. *Osr2* demonstrates expression patterns in the mandibular and maxillary processes, as well as the developing palate, while in the limb buds, it is expressed in the central region of the forelimb mesenchyme, and then follows in the forelimb and hindlimb [11]. Although the exact role of this homolog remains unclear, it was recently reported that a targeted null mutation in *Osr2* impairs palatal shelf growth and causes a delay in palatal shelf

* Corresponding author. Fax: +81 6 6876 8455.
E-mail address: skawai@dent.osaka-u.ac.jp (S. Kawai).

0006-291X/$ - see front matter © 2005 Elsevier Inc. All rights reserved.
doi:10.1016/j.bbrc.2004.12.173

elevation, resulting in cleft palate [13]. While palatal outgrowth initiates normally in the *Osr2* mutant embryos, a significant reduction in palatal mesenchyme proliferation occurs specifically in the medial halves of the downward growing palatal shelves on E13.5, which results in retarded mediolateral symmetric palatal shelves prior to palatal shelf elevation. The developmental timing of palatal growth retardation correlates exactly with the spatiotemporal pattern of *Osr1* gene expression during palate development. In addition, *Osr2* null mice exhibit altered gene expression patterns, including those of *Osr1*, *Pax9*, and *TGFβ3*, during palate development [13]. Therefore, Osr2 is considered likely to play a critical role in the mediation of craniofacial development.

Splicing variants of *Osr2* have been reported in the only available DNA sequence database (GenBank Accession No. AY038074 and NM_054049), however, the exact differences are unknown. In the present study, we cloned and functionally characterized the splicing variants of the *Osr2* gene and found that they have different transcriptional activities. To our knowledge, this is the first direct evidence that gene expression is both positively and negatively regulated by alternative splicing.

Materials and methods

Cell culture. A COS-7 cell line was obtained from Cell Resource Center for Biomedical Research, Tohoku University (Sendai, Japan), and the cells were maintained in Dulbecco's modified Eagle's medium (DMEM) supplemented with 10% fetal calf serum (FCS), 100 U/mL penicillin, and 50 μg/mL streptomycin. C3H10T1/2 cells were purchased from Riken Bioresource Center (Ibaraki, Japan) and maintained in α-modified Eagle's medium (αMEM) supplemented with 10% FCS, 100 U/mL penicillin, and 50 μg/mL streptomycin.

Polymerase chain reaction. Expression analyses of *Osr2* mRNA were performed using Mouse Multiple Tissue cDNA (MTC) panel I (BD Biosciences Clontech, Palo Alto, CA), which contained cDNA from eight types of mouse tissues and four different mouse embryo stages. The primer sets used for the *Osr2* transcript were 5′-CACC ATGGGGAGCAAGGCCTTGCCAGCT-3′ (forward, underlined bases indicate start codon) and 5′-TCAGGCTGTGCCGCCGCAGA TCGC-3′ (reverse, underlined bases indicate stop codon). The polymerase chain reaction (PCR) conditions were 30 cycles at 94 °C for 30 s, 63 °C for 30 s, and 72 °C for 1 min, using *Taq* PCR Master Mix (Qiagen, Hilden, Germany). PCR products (about 0.9 and 0.8 kb) were resolved by electrophoresis on a 1.5% agarose gel. β-Actin was used as an internal control for RNA quantity and the PCR assays.

cDNA cloning and vector construction. Total cellular RNA was prepared using TRIzol reagent and reverse transcribed with SuperScript II reverse transcriptase (Invitrogen, Carlsbad, CA). The primer sets, 5′-CAGATCTCATGGGGAGCAAGGCCTTGCCAG-3′ (forward, underlined bases indicate start codon), and 5′-CGGAATTCCT AGAAGTTCTGCCGCGGGGTG-3′ for *Osr2A* or 5′-TGAATTCTC AGGCTGTGCCGCCGCAGATCG-3′ for *Osr2B* (reverse, underlined bases indicate stop codon), were based on the known coding region sequence of mouse *Osr2* (GenBank Accession No. AY038074 or NM_054049). The forward primer was designed to have a *Bgl*II restriction site, followed by the coding sequence for a Flag epitope in the frame and reverse primers that contained an *Eco*RI site. The PCR conditions were 30 cycles at 94 °C for 30 s, 67 °C for 30 s, and 72 °C for 2 min, with PfuTurbo DNA polymerase (Stratagene, La Jolla, CA). PCR products were digested with *Bgl*II and *Eco*RI, and cloned into *Bam*HI and *Eco*RI-digested pCMV-Tag2A vectors (Stratagene). DNA sequencing was performed using an ABI PRISM 310 Genetic Analyzer (Applied Biosystems, Foster city, CA) and a BigDye Terminator v3.0 Cycle Sequencing Kit (Applied Biosystems). The sequence of the construct was verified by comparing its sequence with that in the DNA sequence database. Gal4 DNA-binding domain (Gal4DBD) fusion proteins were constructed using the *Sal*I and *Mlu*I sites of a pBIND vector (Promega, Madison, WI), with the primer sets 5′-GCGTCGAC TGGGGAGCAAGGCCTTGCCAGC-3′ (forward, underlined bases indicate *Sal*I site), and 5′-CGACGCGTCTAGAAGTTCTGCCGC GGGGTG-3′ for *Osr2A* or 5′-CGACGCGTTCAGGCTGTGCCGC CGCAGATC-3′ for *Osr2B* (reverse, underlined bases indicate *Mlu*I site). The same template cDNA and PCR conditions noted above were applied to construct Gal4DBD-*Osr2* vectors. The 5-kb *Osr2* promoter was amplified by PCR using the primers 5′-AGCGAGAAAGCCTG AGCTCTGCAGGGAAGT-3′ (forward) and 5′-CGGATCCCACCC TCCGGCTGCGAGCGCGCT-3′ (reverse, underlined bases indicate *Bam*HI site used in later cloning) with high fidelity LA *Taq* polymerase (Takara Bio, Shiga, Japan). The amplified product was cloned into a pGL3-basic vector (Promega).

Immunocytochemistry. One day prior to transfection, COS-7 cells were plated on round cover glasses in 24-well culture plates at a density of 4×10^4 per well. The Flag-tagged *Osr2* vector (0.4 μg) was transiently transfected using FuGENE 6 transfection reagent (Roche Molecular Biochemicals, Indianapolis, IN). Approximately 48 h after transfection, the cells were fixed with 3.7% formaldehyde in PBS at room temperature for 10 min, then with 0.1% Triton X-100 in PBS for 10 min and 5% bovine serum albumin (BSA) in PBS for 1 h at room temperature to block non-specific staining. Fixed, permeated, and blocked cells were incubated for 1 h at room temperature with anti-Flag antibody (Stratagene) diluted 1:500 in PBS containing 1% BSA. After rinsing twice in PBS, the cells were incubated at room temperature for 1 h with FITC-conjugated goat anti-mouse IgG (Molecular Probes, Eugene, OR) diluted 1:1000 in PBS–BSA (1%), and then washed twice with PBS. Actin filaments were visualized by rhodamine-conjugated phalloidin (Wako Pure Chemical Industries, Osaka, Japan). Digital photographs of fluorescent sections were taken using an LSM510 laser scanning confocal microscope and analyzed with the included software (Carl Zeiss, Oberkochen, Germany).

Luciferase activity assay. Cells were plated in 24-well culture plates at a density of 4×10^4 per well. After 1 day, the Gal4DBD-*Osr2* vector (0.1 μg) and five Gal4-binding sites containing the firefly luciferase reporter vector, pG5luc (Promega) (0.1 μg), were transiently transfected using FuGENE 6 transfection reagent (Roche Molecular Biochemicals, Indianapolis, IN). *Renilla* luciferase, included in the pBIND vector, was used as an internal control. Approximately 48 h after transfection, the cells were lysed with a passive-lysis buffer, and both firefly and *Renilla* luciferase activities were measured using a Dual Luciferase Reporter Assay System (Promega). The promoter-firefly luciferase activity was normalized by *Renilla* luciferase activity. Each experiment was done in triplicate and repeated at least twice. The *Osr2* promoter-firefly luciferase reporter vector (0.2 μg) was transiently transfected using FuGENE 6 transfection reagent (Roche Molecular Biochemicals) with or without an *Osr2* expression vector. The pRL-CMV vector (20 ng), expressing *Renilla* luciferase and driven by the CMV promoter (Invitrogen), was used as an internal control.

Results and discussion

Genomic structure of Osr2 gene

To obtain the coding region of the mouse *Osr2* gene, we performed an RT-PCR assay and obtained two PCR

products of 0.9 and 0.8 kb. The nucleotide sequencing analysis revealed that this gene encodes proteins with 312 and 276 amino acid residues, respectively, and their difference was observed at the carboxy terminus. We also performed a BLAST search for mouse *Osr2* cDNA (GenBank Accession No. NM_054049) and identified the BAC clone of mouse chromosome 15 (RP24-335P21) containing the *Osr2* gene. A comparison of the cDNA sequences revealed that the *Osr2* gene spans about 7 kb in the genome and consists of 4 exons, as shown in Fig. 1. All sequences of the exon and intron junction follow the acceptor and donor GT-AG rule. Further, *Osr2* variants utilize a different splice acceptor for exon 4 (Table 1).

Additional examination of the database revealed that two variants each for mice, rats, and humans have been deposited in GenBank (Accession No, mouse: AY038074 and NM_054049, rat: XM_235382 and BC079211, and human: AY038072 and AY038073). The long form is termed *Osr2A* and the short form *Osr2B*. *Osr2B* utilized the alternative splice acceptor of 82 bp downstream from splice acceptor in *Osr2A*, causing a frameshift followed by an early stop codon, TAG for *Osr2A* and TGA for *Osr2B* (Fig. 1B). In addition, the Osr2 protein has a zinc-finger motif in the C-terminal half, and motif analyses demonstrated that Osr2A has five zinc-finger domains and Osr2B has three (Fig. 1A).

Tissue distribution of Osr2 variants

To investigate whether alternatively spliced *Osr2* variants are expressed in mouse tissues, we performed PCR analyses with an MTC multiple mouse tissue cDNA panel. Both *Osr2* transcripts were strongly expressed in kidney, muscle, and testis tissues, and at all stages of embryonic development, while it was found weakly in the lung and was not expressed in other types of tissues (Fig. 2). Further, the expression level of *Osr2A* was lower than that of *Osr2B* in those tissues and embryos. The ratio between Osr2A and Osr2B expression was varied among the tissues and embryos, suggesting that Osr2 variants are bifurcated in those sites and situation. Interestingly, all of the tissues that expressed *Osr2* variants were derived from epithelial–mesenchymal interactions. In mouse embryonic development, *Osr2* was detected in kidney, limb buds, mandibular and maxillary arch, and palate tissues [11]. Therefore, we considered that *Osr2* may function in the region of epithelial–mesenchymal interactions during development and in those tissues in adults.

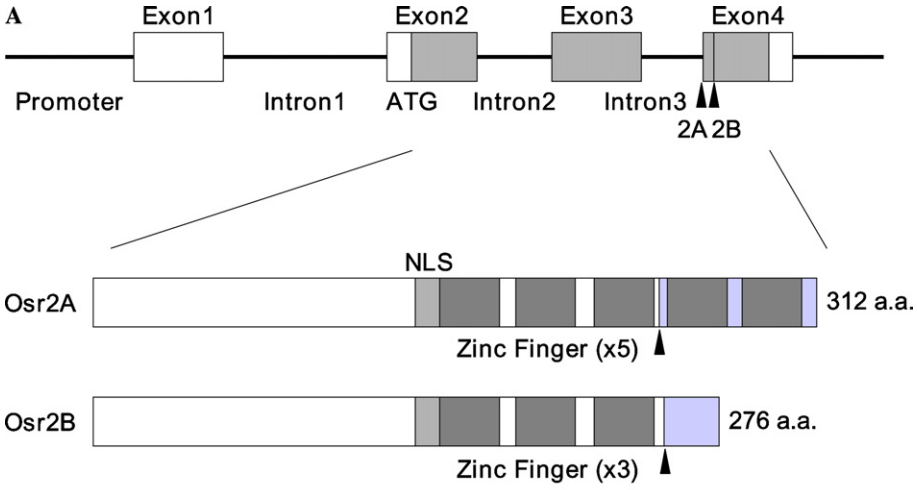

B

```
Osr2A  721 AGGACCCTAGCAGTTCACAAAACTTTACATATGCAGGAATCTCCACACAAATGTCCCACA
Osr2B  721 AGGACCCTAGCAGTTCACAAAACTTTACATATGCAG----------------------

Osr2A  781 TGTGGAAGAACCTTTAATCAGAGAAGTAACCTGAAAACTCACCTTCTCACCCATACAGAC
Osr2B  757 ------------------------------------------------------AC

Osr2A  841 ATCAAGCCCTACAGCTGCGAGCAGTGCGGCAAAGTGTTCAGGCGAAACTGCGATCTGCGG
Osr2B  759 ATCAAGCCCTACAGCTGCGAGCAGTGCGGCAAAGTGTTCAGGCGAAACTGCGATCTGCGG

Osr2A  901 CGGCACAGCCTGACTCACACCCCGCGGCAGAACTTCTAG
Osr2B  819 CGGCACAGCCTGA-------------------------
```

Fig. 1. Schematic representation of *Osr2* splicing variants. (A) Boxes designate exons and gray areas reflect open reading frames, while lines represent the promoter and introns. Both alternative splicing acceptor sites are indicated by arrowheads. A schematic drawing of the zinc-finger domains in Osr2 variants is also shown in the lower portion. Light gray areas denote alternatively spliced exon 4. Osr2A has five zinc-finger domains and Osr2B has three. NLS indicated a putative nuclear localization signal. (B) The alignment of the nucleotide sequence around alternatively spliced exon 4 is shown.

Table 1
Exon–intron splice junctions of the mouse *Osr2* gene

Exon	Size (bp)	Splice acceptor	Splice donor	Intron size (bp)
1	372		GGTTCTGGCG **gt** gagtgtcc	3721
2	767	acactttt **ag** GGATTCCTCT	GGGATCACAG **gt** gaggttgg	956
3	100	tgattttc **ag** GTATATCCAT	ACATATGCAG **gt** aagtttat	725
4a	569	atctgaac **ag** GAATCTCCAC		
4b	487	acccatac **ag** ACATCAAGCC		

Exon and intron sequences are shown in upper- and lowercase letters, respectively. Boldface indicates the GT-AG splice junction sequences in introns.

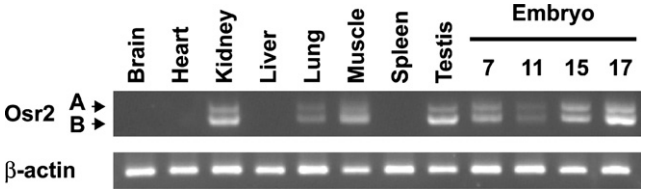

Fig. 2. Tissue distribution of the *Osr2* splicing variants. The *Osr2* transcripts in various tissues were analyzed by PCR. Expression analyses of the *Osr2* mRNA were performed using mouse multiple tissue cDNA (MTC) panel I. Each product (about 0.9 and 0.8 kb) was resolved by electrophoresis on a 1.5% agarose gel. β-Actin was used as the internal control.

Subcellular localization of Osr2 variants

Since both *Osr2* variants were shown to have a putative nuclear localization signal, PSKTKKE, just prior to the zinc-finger domain, subcellular localization of the *Osr2* variants was examined. We transiently expressed Flag-tagged Osr2A and Osr2B in African green monkey kidney COS-7 cells (Fig. 3). As expected, both Osr2A and Osr2B were present in the nuclei and did not show any difference in subcellular localization. This result suggests that Osr2A and Osr2B function in the nucleus as transcription factors with the zinc-finger domain.

Functional analysis of Osr2 activity

Based on the present finding that both *Osr2* variants were localized in the nucleus, we carried out an experiment to determine whether these variants function differently due to the different number of zinc-finger domain repeats. Since the binding DNA sequences of Osr2 remain unclear, we employed a luciferase assay using Gal4DBD-*Osr2* fusion vectors (Fig. 4A) and the Gal4 DNA-binding site of luciferase in COS-7 cells. In cells that transiently expressed Gal4-*Osr2A*, luciferase activity was repressed, while the activity was enhanced in cells transiently expressing Gal4-*Osr2B* (Fig. 4B), showing that Osr2B had a strong transcriptional activity in this system. Next, we screened several promoter-luciferase constructs, including *alkaline phosphatase*, *osteocalcin*, *Runx2*, and *Osr2* (data not shown), and found that the *Osr2* promoter was regulated by *Osr2* gene products (Fig. 5). Osr2A increased *Osr2* promoter activity, whereas Osr2B decreased its activity. It should be noted that the actions of these variants were in reverse of the two luciferase constructs. These results indicate that Osr2 has a regulatory effect on transcriptional activity and its two variants express opposite transcriptional activity in the cells. This behavior seems to be caused by different numbers of zinc-finger domains dependently on

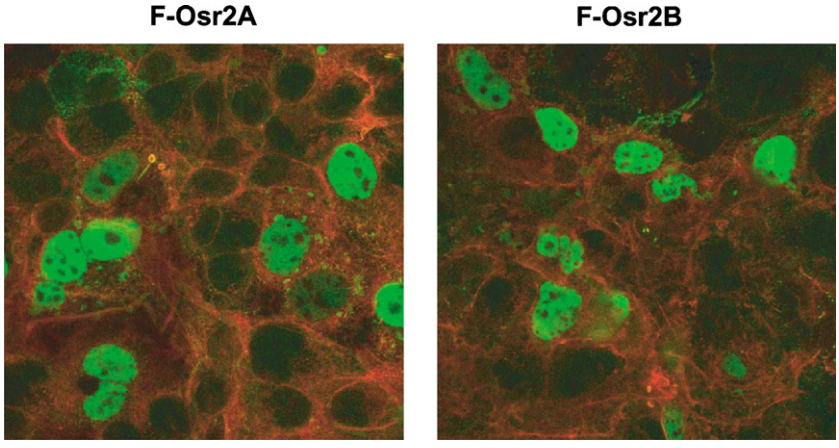

Fig. 3. Subcellular localization of Osr2 proteins. Subcellular localization of Osr2 variants in COS-7 cells was detected by immunocytochemistry. COS7 cells were transfected with a Flag-*Osr2A* or Flag-*Osr2B* vector, then fixed, permeated, and blocked cells were incubated with anti-Flag mouse monoclonal antibody, followed by FITC-conjugated goat anti-mouse IgG (green fluorescence). Actin was stained with rhodamine–phalloidin (red fluorescence) and fluorescence was visualized using a laser scanning confocal microscope.

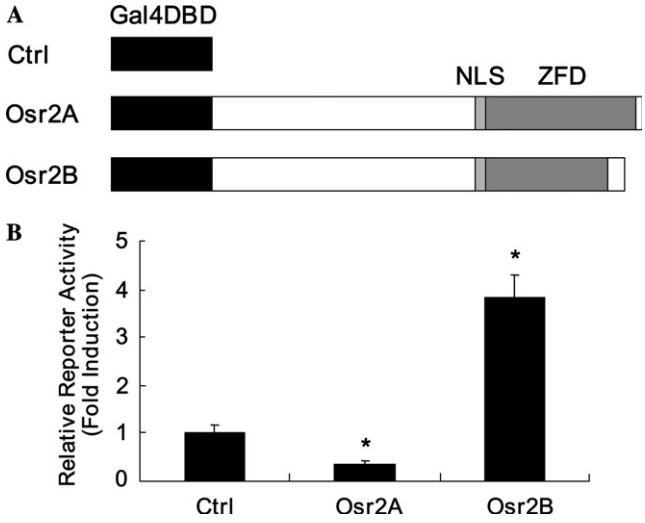

Fig. 4. Transcriptional activity of Gal4DBD-*Osr2* splicing variants in COS-7 cells. Osr2 variants were fused with the Gal4 DNA binding domain (DBD) and transcriptional activity on Gal4 binding sites of the reporter was measured. (A) Constructs of Gal4DBD-Osr2. (B) Relative transcriptional activity. The results are expressed as means ± SD and indicated as *x*-fold induction over the empty vector. Each experiment was performed in triplicate and repeated at least twice. Asterisks indicate the significantly difference ($p < 0.05$) from the mean of control (Ctrl).

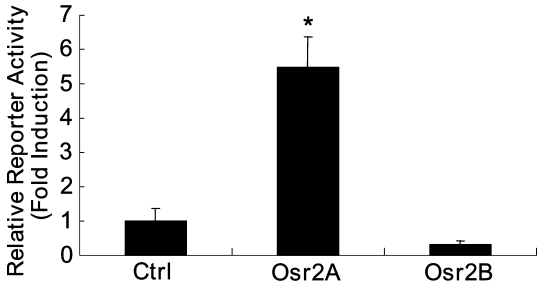

Fig. 5. Regulation of *Osr2* promoter by *Osr2* splicing variants. Osr2 variants and an *Osr2* promoter-luciferase construct were transiently expressed in C3H10T1/2 cells, and then transcriptional activity was measured in the luciferase reporter. The results are expressed as means ± SD and indicated as *x*-fold induction over the empty vector. Each experiment was performed in triplicate and repeated at least twice. Asterisks indicate the significantly difference ($p < 0.05$) from the mean of control (Ctrl).

the target genes and cells. No evidence is available to explain this finding at this moment, however, these zinc-finger domains may be differently modified such as phosphorylation and/or show different affinity for DNA binding, resulting in opposite transcriptional function.

In the present study, we characterized the structural organization of the *Osr2* gene and found the existence of two transcripts that are generated by alternative splicing of different splice acceptor sites for exon 4. The Osr2 variants were shown to have opposite transcriptional activity, indicating that the function of Osr2 is regulated by alternative splicing. The splicing variants were detected in several tissues and embryos, and confirmed to be localized in the nucleus. Osr2 might have important functions in epithelial–mesenchymal interactions throughout the development. Hardy et al. [14] reported that the mouse *interleukin-1 receptor-associated kinase 2* (*IRAK2*) gene encodes four alternatively spliced isoforms, two of which have a stimulatory effect on NF-κB activation, while the others are inhibitory. Ando et al. [15] also found that *LIM homeodomain protein Islet-1* (*Isl1*) has 2 splicing variants and *Isl1β* was a relatively more potent transcriptional activator of the insulin promoter than *Isl1α*. The transcriptional activity of *Isl1* is potentially regulated by the alternative splicing of its mRNA. From these previous findings, it is expected that *Osr2* variants have an individual function in embryonic development, such as in epithelial–mesenchymal interactions. Further, *Osr2* has been reported to be expressed in mandibular and maxillary mesenchyme tissues, while *Osr2*-deficient mice exhibited cleft palate and altered gene expression patterns of *Osr1*, *Pax9*, and *TGFβ3* [13]. In future studies, it is necessary for the function of splicing variants to be elucidated in the mandible, maxillary, and palate, as well as teeth. It is also needed to examine how the variants are chosen and share their roles in the developmental process.

The human and nematoda genomes have nearly the same number of genes (approximately 22,000 and 19,000, respectively) [7,16], though the human genome exhibits considerably more variations and complexity than that of nematoda. Alternative splicing may provide an important contribution to the understanding of such complex processes as gene function and lead to the development of strategies to increase the functional multiplicity of a limited number of genes.

Acknowledgments

This study was supported in part by Grants-in-Aid for Scientific Research from the Japanese Society for the Promotion of Science (No. 15390645). This work was a part of the 21st Century COE entitled "Origination of Frontier BioDentistry" at Osaka University Graduate School of Dentistry, supported by the Ministry of Education, Culture, Sports, Science and Technology.

References

[1] M.C. Hart, L. Wang, D.E. Coulter, Genetics 144 (1996) 171–182.
[2] D.E. Coulter, E.A. Swaykus, M.A. Beran-Koehn, D. Goldberg, E. Wieschaus, P. Schedl, EMBO J. 9 (1990) 3795–3804.
[3] A.S. Manoukian, H.M. Krause, Development 118 (1993) 785–796.
[4] D.E. Coulter, E. Wieschaus, Genes Dev. 2 (1988) 1812–1823.
[5] S. DiNardo, P.H. O'Farrell, Genes Dev. 1 (1987) 1212–1225.
[6] J.R. Mullen, S. DiNardo, Dev. Biol. 169 (1995) 295–308.

[7] The Washington University Genome Sequencing Center, Science 282 (1998) 2012–2018.
[8] S. Brohl, T. Lisowsky, G. Riemen, G. Michaelis, Yeast 10 (1994) 719–731.
[9] S.L. Klein, R.L. Strausberg, L. Wagner, J. Pontius, S.W. Clifton, P. Richardson, Dev. Dyn. 225 (2002) 384–391.
[10] P.L. So, P.S. Danielian, Mech. Dev. 84 (1999) 157–160.
[11] Y. Lan, P.D. Kingsley, E.S. Cho, R. Jiang, Mech. Dev. 107 (2001) 175–179.
[12] M. Katoh, Int. J. Mol. Med. 10 (2002) 221–225.
[13] Y. Lan, C.E. Ovitt, E.S. Cho, K.M. Maltby, Q. Wang, R. Jiang, Development 131 (2004) 3207–3216.
[14] M.P. Hardy, L.A. O'Neill, J. Biol. Chem. 279 (2004) 27699–27708.
[15] K. Ando, S. Shioda, H. Handa, K. Kataoka, J. Mol. Endocrinol. 31 (2003) 419–425.
[16] International Human Genome Sequencing Consortium, Nature 431 (2004) 931–945.